










Electrical and mechanical properties of poly(dopamine)-modified copper/reduced graphene oxide composites

Zhengfeng Jia^{1,2,3} , Haoqi Li² , Yao Zhao² , Laszlo Frazer⁴ , Bosen Qian² , Eric Borguet⁴ , Fei Ren^{2,*} , and Dmitriy A. Dikin^{2,*} 

¹ College of Materials Science and Engineering, Liaocheng University, Liaocheng 252059, People's Republic of China

² Department of Mechanical Engineering, Temple University, Philadelphia, PA 19122, USA

³ State Key Laboratory of Solid Lubrication, Lanzhou Institute of Chemical Physics, Chinese Academy of Sciences, Lanzhou 73000, People's Republic of China

⁴ Department of Chemistry, Temple University, Philadelphia, PA 19122, USA

Received: 26 October 2016

Accepted: 17 June 2017

Published online:

23 June 2017

© Springer Science+Business Media, LLC 2017

ABSTRACT

Surface oxidation is frequently encountered in powder metallurgy of metals and alloys, and it leads to a reduction in their electrical conductivities. Therefore, it is highly desired to remove the naturally occurring oxide layer from the particles surface and to prevent its subsequent formation. A new approach was proposed in this study, where copper particles were mixed with graphene oxide (GO) sheets in an aqueous solution containing dopamine (DA) molecules. It was expected that polymerization of the DA molecules on the surface of the copper particle could promote both a reduction of surface oxide layer and the adhesion of GO sheets to the particles surface. The powder system was then washed, heat-treated in inert atmosphere and compressed at room temperature to form compacts. Electron microscopy revealed nearly ideal dispersion of GO sheets within the copper matrix. X-ray photoelectron spectroscopy showed a shift from Cu^{2+} to Cu^+ and metallic copper in the coated and heat-treated samples, and Raman spectroscopy pointed to the increased amount of sp^2 carbon as a result of the heat treatment. All DA/GO-coated and heat-treated compacts exhibited significantly higher electrical conductivity than those that have been made from pure copper powder or were not been heat-treated. Also, indentation measurements showed an increase in microhardness in samples with the shortest, 10 min, coating time and heat-treated at the highest, 600 °C, temperature.

Address correspondence to E-mail: renfei@temple.edu; ddikin@temple.edu

Introduction

Most of actual metal powders consist of oxide-covered particles, which complicate their effective use and increase costs of application. Removing oxides, preserving the surface of metal powder for easy handling and their technological utilization in any type of environment would be a valuable step toward cost reduction and improvement in existing or developing of new products. Graphene sheet, one-atom-thick sp^2 -bonded network of carbon atoms, in combination with effective reduction chemistry of graphene oxide, could possibly serve this purpose. Graphene itself has excellent electrical, thermal and mechanical properties, which when used as additives to other matrices may enhance the performance of the composite materials [1, 2]. However, mass production of graphene sheets is very expensive. Instead, reduced graphene oxide (rGO), obtained by chemical reduction of graphene oxide, is often used as a substitute to graphene due to the similar properties. Sheets of rGO have good manufacturing scalability and, therefore, are relatively inexpensive. Although rGO sheets comprise some residual oxygen-containing functional groups, their physical properties are greatly approaching the properties of pristine graphene sheets [3], considering their high aspect ratio and easy dispersion in a variety of solvents may serve the purpose of nanofillers in many composite materials for large-scale engineering applications.

Metal/rGO composites can be fabricated using various methods, including electrochemical synthesis, simultaneous chemical reduction of graphene oxide (GO) and metal ions, microwave-assisted synthesis and other techniques [4]. Recently, Jia and coworkers synthesized rGO/Cu composites by in situ reduction of GO and Cu^{2+} to enhance adhesion between rGO and Cu nanoparticles [5]. While introduction of rGO into a metal matrix may enhance the mechanical strength [6, 7] of composite structures, there is limited information about changes in the electrical conductivity of highly conductive metallic powders such as Cu and Al. One exception is the recently reported synthesis of Cu/Covetic nanostructured composites prepared by stirring carbon nanotubes into molten metal in the presence of a high direct current [8, 9]. Their enhanced electrical conductivity is explained as a result of the covalent/metallic bonding between carbon nanoinclusions and the metal matrix.

In this work, we fabricated copper powder matrix composites by room temperature compaction of poly(dopamine) (PDA)-modified and rGO-coated copper powder. A single-pot mixing of microsize Cu particles and GO sheets was conducted in the dopamine (DA) aqueous solution. It is known [10] that under mild basic conditions DA molecules are polymerized and form thin films on various surfaces through a self-assembly process. The presence of amine ($-NH_2$) and hydroxyl ($-OH$) functional groups in PDA molecules promotes their strong adhesion to both organic and inorganic material surfaces [11, 12]. In addition, the polymerization of DA is an oxidative process and may lead to a simultaneous reduction of metal ions and graphene oxide sheets [13, 14]. Therefore, in our approach we hoped to use this reaction to achieve polymerization of DA with the concurrent removal of copper oxide, reduction of GO sheets, and assist the adhesion of rGO to the surface of Cu particles. In the next step, before compaction, we heat-treated the composite powder, and the PDA coating could be carbonized or even partially graphitized depending on the temperature and other conditions [15], and GO sheets will be additionally reduced.

Materials and method

In this study, Cu powder (>99% pure, 14–25 μm), dopamine hydrochloride (both from Sigma-Aldrich, St. Louis, MO, USA) and GO water dispersion (4 mg mL^{-1} , Graphenea SA, Spain) were purchased and used without further treatment. According to the manufacturer's analysis, the carbon-to-oxygen ratio in the GO is 1.2:1 with the remaining nitrogen <1% and sulfur <2%. To prepare the dopamine Tris solution, Tris(hydroxymethyl) aminomethane (Sigma-Aldrich, St. Louis, MO, USA) was initially mixed with deionized water and HCl was dropped into solution to balance the pH value to 8.5. Dopamine hydrochloride powder (Sigma-Aldrich, St. Louis, MO, USA) was then dissolved in the Tris buffer to the concentration of 50 mM. In a typical coating trial, 10 g of Cu powder and 3 mL of GO suspension were simultaneously mechanically stirred into 50 mL of the 50-mM dopamine Tris solution at room temperature, which also corresponds to approximately 0.24 mg mL^{-1} concentration of GO sheets in water, and 0.12 wt% of GO nanosheets in relation to Cu

powder. At this concentration, the GO monolayer content has to be more than 95%. A representative scanning electron microscopy image of GO sheets deposited on the silicon substrate is shown in Figure S1 (supplementary information). This mixture was continuously stirred using magnetic stir bars for a given time ($t = 10$ min, 1 or 48 h). The powder was then separated by centrifugation and cleaned with deionized water. The centrifuging and cleaning were repeated at least three times before the powder was dried at 50 °C in air using a laboratory oven for 3 h.

The thermogravimetric analysis (TGA) (Pyris 6 TGA under N₂ atmosphere) of pure PDA powder showed gradual weight loss during the pyrolysis process with a slowing down around 470–500 °C (Fig. 1a). Therefore, in this work, we chose to heat-treat the dried powder at 500 and 600 °C in a tube furnace with the flowing Ar for 0.5 h. Cu/GO/PDA composite powder and pure Cu powder, both heat-treated at the same conditions, were uniaxially compressed at room temperature and 475 MPa into disk-shaped pellets having 12.7 mm diameter and about 2 mm thickness.

The density of the pellets was determined using the Archimedes' method in isopropyl alcohol (99%, from Sigma-Aldrich) to ensure good wettability of the surface and no air bubbles. The morphology of the loose powders and pellets was examined using scanning electron microscopy (SEM FEI QUANTA 450FEG). X-ray diffraction (XRD) measurements were taken using a Bruker D8 X-ray diffractometer with Cu K_α radiation (wave length = 1.5405 Å). X-ray photoelectron spectroscopy (XPS) was performed on a VGESCALAB MKII spectrometer operated at 25 kV. Confocal Raman spectroscopy was conducted using a Horiba LabRam HR evolution spectrometer with a 532-nm laser. Electrical conductivity was calculated based on the sample geometry and resistance measured using a 4-probe configuration.

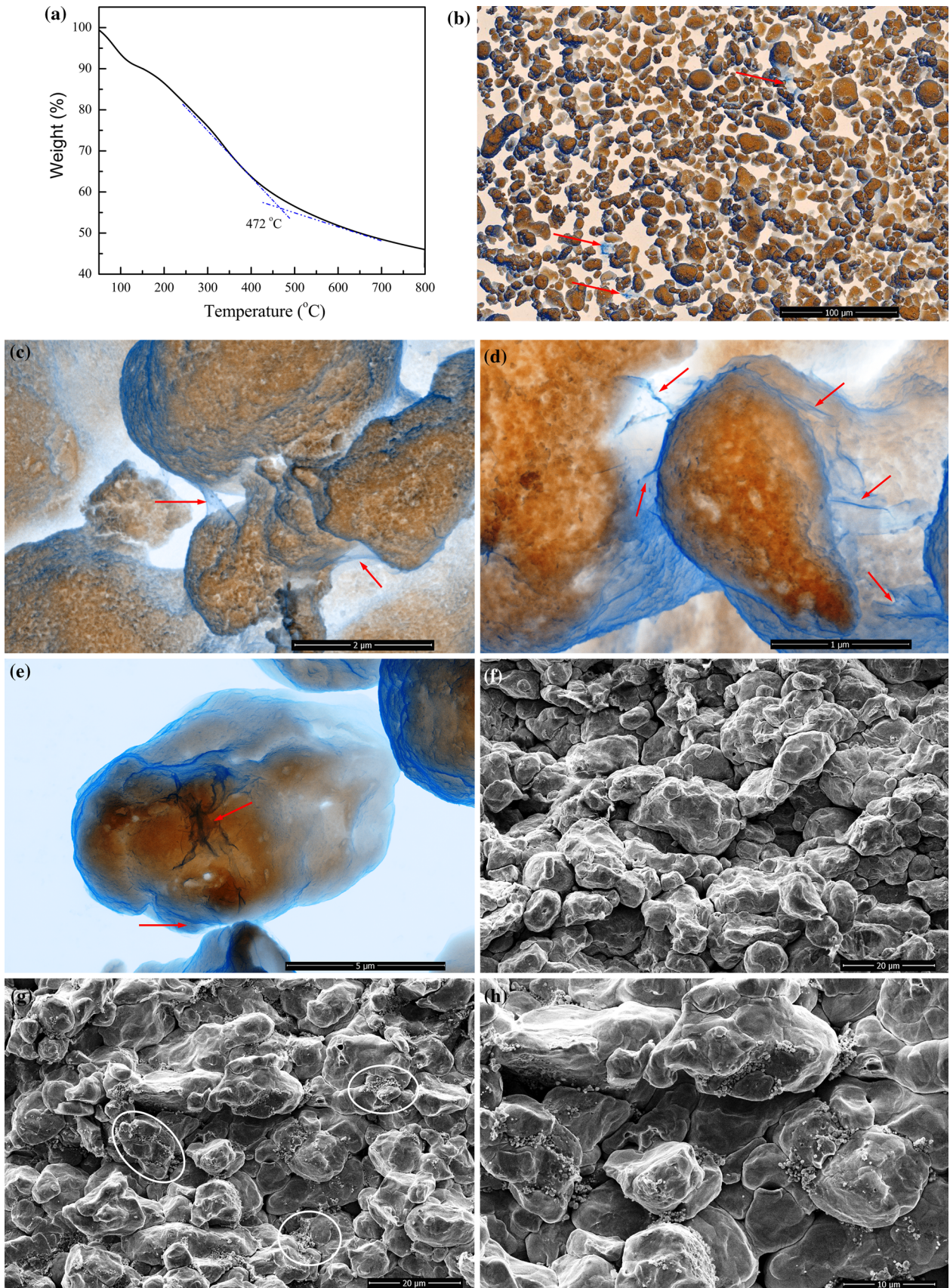
Microhardness was measured on the flat surfaces of the pellets using a Wilson/Tukon microhardness tester equipped with a Vickers indenter tip. During a trial run, the loading force was increased from 0.98 to 9.8 N. Measured hardness values initially decreased with increasing load and then remained unchanged above 2.94 N. The loading force was fixed at 9.8 N for all samples in order to include as many copper grains as possible in an individual indentation test. At this load, the size of the indent impressions ranged between 120 and 230 μm. The loading time was fixed

at 10 s. At least nine indents were performed on each sample. To obtain the microhardness value, the following equation was applied: $HV = 1.8544F/d^2$, where F is applied load, d is the average length of the two indent diagonals.

Results and discussion

Due to the hydrophilic nature of GO, the exfoliated sheets can stay in the water solution for indefinite time without precipitation even at relatively high concentration of 4 mg mL⁻¹. Using 3 mL of GO solution for one batch and mixing it with 10 g of Cu powder in 50 mL of Tris buffer (0.12 wt% of GO in Cu), we expect to obtain approximately 8 m² of the total GO surface area, if this material is exfoliated down to individual sheets and assuming its 0.8 nm [16] thickness and 1.8 g cm⁻³ density. At the same time, 10 g of Cu powder has approximately 0.8 m² of surface area assuming the monosized spherical particles to be 20 μm in diameter and that the bulk density of Cu is 8.96 g cm⁻³. The ratio between estimated surface area of GO sheets and that of Cu particles is approximately 10:1, which allows us to hope in adequate total coverage of metal particles with graphene oxide.

Figure 1b–e shows representative SEM images of the Cu/GO/PDA composite powder particles. Due to its nanometer thickness and high transparency for electron beam, it is impossible to see the GO sheets at low magnification except in cases when they form aggregates, as it is marked with red arrows in Fig. 1b. At much higher magnification, e.g., 50 kX and above (Fig. 1c–e), one can see that Cu particles are indeed wrapped in the GO sheets as evidenced by the characteristic wrinkles or partially freestanding layers. Based on literature information [10], it is believed that under the current synthesis conditions the polymerized DA forms a nanometer-thick film on the Cu surface due to its excellent adhesion ability and also provides much needed extensive adhesion of the GO sheets. Unfortunately, thin film of PDA cannot be seen directly using the SEM imaging technique as well. Nevertheless, focusing a steady electron beam at a single spot, we can observe slight morphological changes, such as minor swelling, ablation, redepositing, on the Cu surface in case if this sample has not been heat-treated. This is indicative of the presence of a thin polymer film.



◀ **Figure 1 a** Thermogravimetric analysis (TGA) curve of pure PDA powder recorded in nitrogen gas atmosphere with a scan rate $10\text{ }^{\circ}\text{C min}^{-1}$, **b–e** SEM images of loose copper particles mixed with PDA and GO for 10 min, washed, centrifuged and dried at room temperature. All images are in false colors produced as a mixture of signals from the secondary (ETD) and the backscatter (CBS) electron detectors; ETD SEM images, **f** of the fractured surface of the composite Cu/PDA/GO samples unheated and, **g** and **h** heat-treated at $600\text{ }^{\circ}\text{C}$ and, **i** at $500\text{ }^{\circ}\text{C}$. **f** and **g** Images are taken at the same magnification.

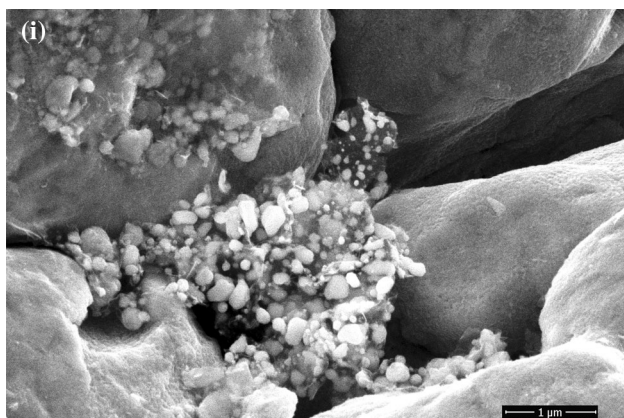


Figure 1 continued.

Figure 1f, g shows the fractured surface of compressed pellets made from the composite powder without and with the heat treatment at $600\text{ }^{\circ}\text{C}$. Primarily, the intergranular fracture is evident in these images, as well as significant plastic deformation of the Cu particles leading to their partial coalescence/sintering. During the powder compression, the obvious elastic deformation, rearrangement and the partial fragmentation of the particles take place before the major plastic deformation. The whole process of compaction should also be accompanied by the shear deformations along particle contacts and break of the remaining copper oxide layer [17, 18] and GO/PDA films. This allows formation of metal-to-metal contacts and increase in electrical conductivity, which will be discussed later.

As a result of the heat treatment, the GO sheets are reduced forming rGO [19], and the PDA film is carbonized forming cPDA. Again, at low magnification in Figs. 1f, g we cannot see rGO sheets. However, in the case of heat-treated powder (Fig. 1g), we noticed the appearance of sub-micrometer size particles at

many locations, which are visible even at relatively low magnification and are outlined in the figure. Higher magnification SEM images (Fig. 1h, i) revealed that these particles are attached to both sides of “free” standing rGO sheets and filling the voids between large Cu particles. They are not observed in the samples of the same composition that have not undergone heat treatment (Fig. 1f and Figure S2). The energy-dispersive x-ray spectroscopy (EDS, Figure S3) indicates that these particles are composed of Cu and enriched amount of C and O, as expected, but the exact compositional ratio cannot be assessed due to the strong material inhomogeneity within the volume of its interaction with an electron beam (see supplementary information). Currently, we can only speculate that these nanoparticles, consisting of copper oxide and collected together with rGO sheets and cPDA, are removed sheathing, which is initially formed on the Cu oxide surface coated with GO/PDA, as a result of plastic and shear deformation and some sort of migration of these slag formations into available intergranular pockets. Noticeably, they are not observed on the fracture surface of samples having the same composition but not heat-treated. Additional experimental work has to be carried out in order to understand the nature and the formation mechanism of these particles.

The Raman spectra of the Cu/GO/PDA composite samples (Fig. 2a) show two broad and low intensity peaks around 1350 and 1570 cm^{-1} in all three samples. These two peaks are identified as the D band ($\sim 1350\text{ cm}^{-1}$) due to sp^3 carbon and the G band ($\sim 1570\text{ cm}^{-1}$) associated with sp^2 hybridization of carbon atoms (e.g., in graphite) [14, 20, 21]. With heat treatment, both the D and G peaks became more prominent, implying that the concentration of the sp^2 and sp^3 carbons slightly increased. The intensity ratio between the D and G bands (I_D/I_G), which is related to the graphitization degree of carbonaceous materials and the defect density, slightly increased after heat treatment at $600\text{ }^{\circ}\text{C}$, possibly suggesting the creation of new small sp^3 domains due to the pyrolysis of PDA [15, 20, 22, 23]. A comparison of the XRD spectra is shown in Fig. 2b where the (111), (200) and (220) peaks of Cu are registered [20], but the characteristic graphite peak was not observed implying either no multi-layer graphite or that it may be in too low a concentration to be detectable.

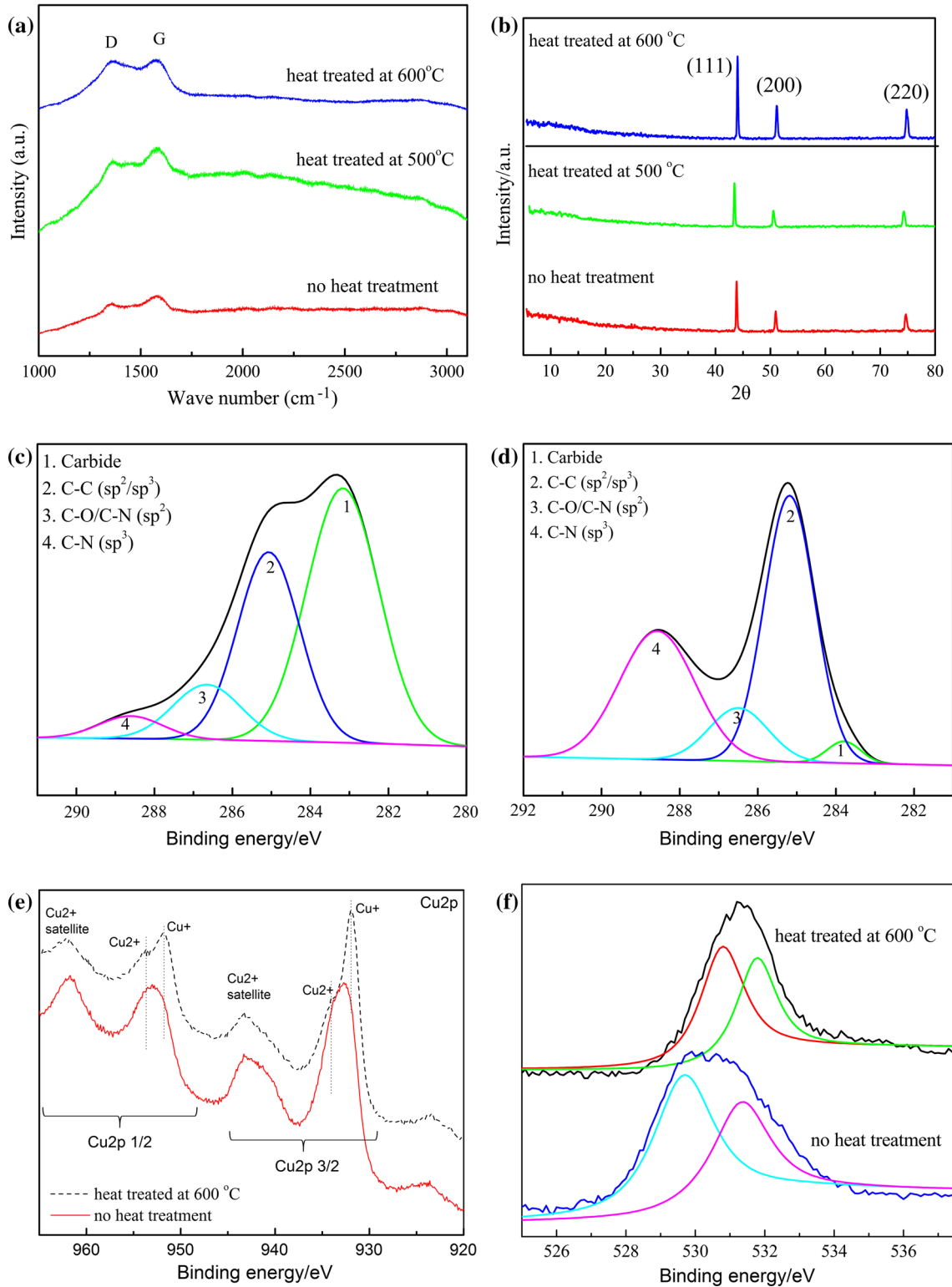


Figure 2 a Raman and b XRD spectra for composite powders before and after heat treatments at 500 and 600 °C, c XPS high resolution C1s spectra for Cu/GO/PDA before and d after heat

treatment at 600 °C, e XPS Cu2p spectra and f XPS high resolution O1s for unheated Cu/GO/PDA and Cu/rGO/cPDA after heat treatment at 600 °C.

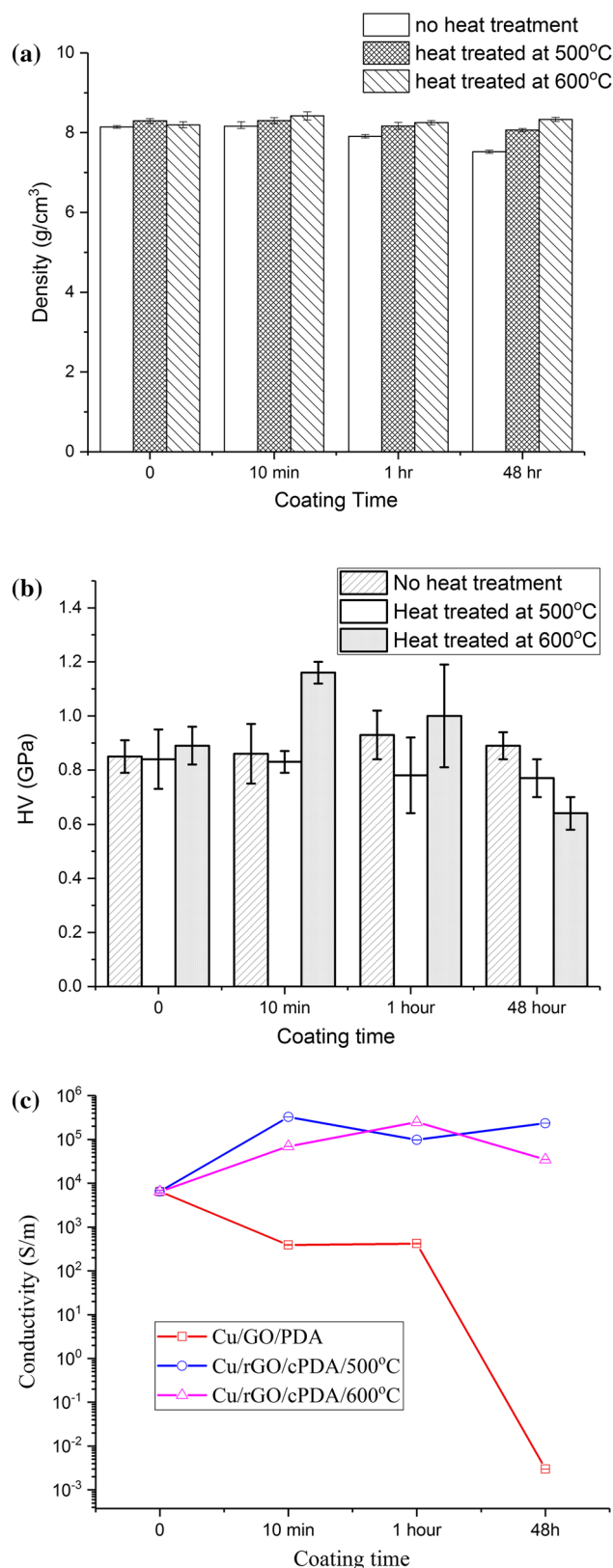


Figure 3 a Density, b microhardness and c electrical conductivity of compressed powder samples as a function of processing conditions. Lines connecting data points are only as a guide to the eye. a, the errors in density measurements ranged from 0.03 to 0.11 g/cm³, which corresponding to 0.3 to 1.2% of relative density. In all figures, data of compressed pure copper powder are indicated as “0” coating time.

Figure 2c, d presents the XPS spectra of the Cu/GO/PDA composite samples collected before and after heat treatment at 600 °C. Based on the deconvolution of the C1s peak, the peak centered at 283.2 eV is attributed to carbide, implying that chemical reaction occurred between Cu and PDA (Fig. 2c) [24, 25]. The peaks at 285.2, 286.5 and 288.5 eV can be attributed to C–C (*sp*² and *sp*³), C–O/C–N (*sp*²) and C–N (*sp*³) bonds, respectively, in dopamine derivatives and some remaining oxygen-containing groups of rGO [21]. Comparing the two profiles, the carbide peak at 283.2 eV was weakened and the peaks at 285.2 and 288.5 eV became stronger after pyrolysis, which implies that the amount of carbide decreased while those of the carbon and C–N (*sp*³) bonds increased as a result of carbonization of PDA and transformation of GO to rGO that removes the majority of oxygen-containing functional groups [16, 26]. Deconvolution of the O1s peak of the sample without heat treatment shows (see Fig. 2f) two peaks at 529.7 and 531.2 eV, which are attributed to the oxides of copper and organic C–O, respectively [9, 24]. After heat treatment at 600 °C, the peak at 529.7 eV shifted to 530.8 eV, implying the mixture of copper oxides and organic C–O; and the peak at 531.2 eV shifted to 532.2 eV, indicating transformation from C–O to C=O, implying that reduction of the oxygen atoms in PDA and GO occurred (Fig. 2f) [25, 26]. Therefore, it may be concluded that the PDA was transferred into N-doped carbon-containing material and the GO nanosheets were reduced into rGO nanosheets during heat treatment. Figure 2e compares the XPS Cu2p spectra of samples with and without heat treatment at 600 °C. Cu2p 3/2 and Cu2p 1/2 spectral peaks indicate the presence of both the Cu²⁺ (~934 eV) and the Cu⁺ (~932 eV) states of copper coordination in the heat-treated and untreated samples. Wherein, a shift toward Cu⁺ in heat-treated material is evident, indicating a

transformation to Cu_2O and/or metallic copper and suppression of CuO . There is also a possibility to form copper acetylide Cu_2C_2 .

Density measurements of the compressed pellets are shown in Fig. 3a. One-hour and especially 48-h coated unheated composite samples display the lowest density, which is due to relatively large amount of polymer component. At the same time, heat-treated composites having significantly reduced volume of PDA as a result of carbonization (see the TGA curve in Fig. 1a) may facilitate a better sliding and packing of copper particles during the compaction, which apparently leads to a slight increase in the packing density of composites even with an initially large amount of PDA. The amount of PDA and, later, cPDA and GO and correspondingly rGO in the 10-min coated composites are very small in all cases, and if for unheated composites its presence does not affect the packing density, while in the case of heat-treated composites we observed small increase in the packing density from 91% to about 94%, assuming that the bulk density of copper is 8.96 g cm^{-3} .

The results of Vickers microhardness data are shown in Fig. 3b. In this study, all samples were tested with a load of 9.8 N and the indent size ranged between 120 and 230 μm , corresponding to penetrations ranging between 48 and 93 μm , which were at least twice the size of the copper particle (14–25 μm). Therefore, the measured data represented the hardness of the bulk materials. The Cu/PDA/GO sample with 10-min coating and 600 °C heat treatment, the thinnest layer of cPDA and rGO, exhibited the highest hardness of $1.16 \pm 0.04 \text{ GPa}$. On the other hand, the sample with 48 h coating and 600 °C heat treatment had the lowest hardness of $0.64 \pm 0.06 \text{ GPa}$, which might be due to the fact that large amount of PDA leaves a relatively thick carbonized layers hindering connections between Cu particles during the compaction. Combining these results with the density measurements, we can conclude that thin coating layer, 10-min treatment with 600 °C heating, leads to the best combination of packing and composite hardness. Considering the uncertainty in the data (Fig. 3b), no significant differences could be identified between the Cu and Cu/PDA/GO samples processed using other conditions.

The room temperature electrical conductivity shows strong dependence on the processing conditions, such as coating time and heat treatment (Fig. 3c). For samples without heat treatment, the

electrical conductivity decreased as the coating time increased. This is due to the non-conducting nature of PDA and GO that form dielectric layers on the Cu particles. However, after the heat treatment the electrical conductivity of the composite samples out-performed their pure Cu counterparts by about 100 times (Fig. 3c). The electrical conductivity of the compact sample of the pure copper powder is $(6.5 \pm 0.5) \times 10^3 \text{ S m}^{-1}$, while the electrical conductivity of heat-treated Cu/GO/PDA composite samples was as high as $(3.3 \pm 0.5) \times 10^5 \text{ S m}^{-1}$ (Fig. 3c). A possible explanation is that the processing method developed in this study, PDA/GO coating and heat treatment, can remove the surface oxide from the Cu particles [25], while the PDA and GO were, respectively, converted to carbonized cPDA and rGO, thus increasing the electrical conductivity of the powder compact. This hypothesis is at least partially supported by the previously discussed XPS and Raman results, which show a formation of graphitized PDA and the chemical bonding between copper and cPDA. Heat treatments at both 500 and 600 °C seemed to give comparable results. A coating time longer than 10 min did not provide additional benefits. Therefore, from an engineering point of view, a coating time of c.a. 10 min followed by the heat treatment at 600 °C can serve as an effective means to increase the electrical conductivity and mechanical hardness of copper powder matrix composite.

Conclusions

In this work, a single-pot processing method is developed to fabricate copper/carbon composite powders by the dopamine stimulated coating of copper particles with graphene oxide sheets in aqua suspensions followed by heat treatment at 500 and 600 °C in inert atmosphere. The solid samples fabricated by compressing the composite powder at room temperature exhibited almost no signs of aggregated carbon. A short duration of coating in dopamine-graphene oxide solution and subsequent heat treatment improved the compaction density and enhanced the mechanical hardness and the electrical conductivity of the resulting composite. Thus, the formation of poly(dopamine), in addition to a heat treatment, helped the reduction of GO as well as the reduction of surface oxide on the Cu particles

contributing to a decrease in the grain boundary electrical resistance and promoting their adhesion.

Acknowledgements

ZFJ thanks the support of Project of Shandong Province Higher Educational Science and Technology Program of China (No. J15LA60) and Open Project of State Key Laboratory of Solid Lubrication, Lanzhou Institute of Chemical Physics, China (LSL-1504). FR would like to acknowledge financial support from the Temple University faculty startup fund. The SEM imaging was performed in the CoE-NIC facility at Temple University, which is based on DoD DURIP Award N0014-12-1-0777 from the Office of Naval Research and is sponsored by the College of Engineering. EB and LF acknowledge support as part of the Center for the Computational Design of Functional Layered Materials, an Energy Frontier Research Center funded by the US Department of Energy, Office of Science, Basic Energy Sciences under Award#DE-SC0012575.

Electronic supplementary material: The online version of this article (doi:[10.1007/s10853-017-1307-z](https://doi.org/10.1007/s10853-017-1307-z)) contains supplementary material, which is available to authorized users.

References

- [1] Weiss NO, Zhou HL, Liao L, Liu Y, Jiang S, Huang Y, Duan XF (2012) Graphene: an emerging electronic material. *Adv Mater* 24:5782–5825
- [2] Geim AK (2009) Graphene, status and prospects. *Science* 324:1530–1534
- [3] Whitby RLD (2014) Chemical control of graphene architecture: tailoring shape and properties. *ACS Nano* 8:9733–9754
- [4] Huang X, Yin Z, Wu S, Qi X, He Q, Zhang Q, Yan Q, Boey F, Zhang H (2011) Graphene-based materials: synthesis, characterization, properties, and applications. *Small* 7:1876–1902
- [5] Jia Z, Chen T, Wang J, Ni J, Li H, Shao X (2015) Synthesis, characterization and tribological properties of Cu/reduced graphene oxide composites. *Tribol Int* 88:17–24
- [6] Hwang J, Yoon T, Jin S, Lee J, Kim T, Hong S, Jeon S (2013) Enhanced mechanical properties of graphene/copper nanocomposites using a molecular-level mixing process. *Adv Mater* 25:6724–6729
- [7] Ma D, Wu P (2016) Improved microstructure and mechanical properties for Sn58Bi0.7Zn solder joint by addition of graphene nanosheets. *J Alloy Compd* 671:127–136
- [8] Isaacs RA, Zhu H, Preston C, Mansour A, LeMieux M, Zavalij PY, Iftekhar Jaim HM, Rabin O, Hu L, Salamanca-Riba LG (2015) Nanocarbon-copper thin film as transparent electrode. *Appl Phys Lett* 10(1063/1):4921263
- [9] Knych T, Kiesiewicz G, Kwaśniewski P, Mamala A, Kawecki A, Smyrak B (2014) Fabrication and cold drawing of copper covetic nanostructured carbon composites. *Arch Metall Mater*. doi:[10.2478/amm-2014-0219](https://doi.org/10.2478/amm-2014-0219)
- [10] Lee H, Dellatore SM, Miller WM, Messersmith PB (2007) Mussel-inspired surface chemistry for multifunctional coatings. *Science* 318:426–430
- [11] Cui W, Li M, Liu J, Wang B, Zhang C, Jiang L, Cheng Q (2014) A strong integrated strength and toughness artificial nacre based on dopamine cross-linked graphene oxide. *ACS Nano* 9:9511–9517
- [12] Krogsgaard M, Nue V, Birkedal H (2016) Mussel-inspired materials: self-healing through coordination chemistry. *Chem Eur J* 22:844–857
- [13] Wahrmond J, Kim J, Chu L, Wang C, Li Y, Fernandez-Nieves A, Weitz DA, Krokhn A, Hu ZB (2009) Swelling kinetics of a microgel shell. *Macromolecules* 42:9357–9365
- [14] Fu Y, Li P, Xie Q, Xu X, Lei L, Chen C, Zou C, Deng W, Yao S (2009) One-pot preparation of polymer-enzyme-metallic nanoparticle composite films for high-performance biosensing of glucose and galactose. *Adv Funct Mater* 19:1784–1791
- [15] Ryu S, Chou J, Lee K, Lee D, Hong S, Zhao R, Lee H, Kim SG (2015) Direct insulation-to-conduction transformation of adhesive catecholamine for simultaneous increases of electrical conductivity and mechanical strength of CNT fibers. *Adv Mater* 27:3250–3255
- [16] Stankovich S, Dikin DA, Piner RD, Kohlhaas KA, Ijehammas A, Jia Y, Wu Y, Nguyen S, Ruoff RS (2007) Synthesis of graphene-based nanosheets via chemical reduction of exfoliated graphite oxide. *Carbon* 45:1558–1565
- [17] Montes JM, Cuevas FG, Cintas J (2010) Analytical theory for the description of powder systems under compression. *Appl Phys A* 99:751–761
- [18] Montes JM, Cuevas FG, Cintas J (2007) Electrical resistivity of metal powder aggregates. *Metall Mater Trans B* 38B:957–964
- [19] Renteria JD, Ramirez S, Malekpour H, Alonso B, Centeno A, Zurutuza A, Ccemasov AI, Nika DL, Balandin AA (2015) Strongly anisotropic thermal conductivity of free-standing reduced graphene oxide films annealed at high

- temperature. *Adv Funct Mater.* doi:[10.1002/adfm.201501429](https://doi.org/10.1002/adfm.201501429)
- [20] Cao H, Wang Y, Xiao F, Ching C, Duan H (2012) Growth of copper nanotubes on graphene paper as free-standing electrodes for direct hydrazine fuel cells. *J Phys Chem C* 116:7719–7725
- [21] Kaminska I, Qi W, Barras A, Sobczak J, Niedziolka-Jonsson J, Woisel P, Lyskawa J, Laure W, Opallo M, Li M, Boukherroub R, Szunerits S (2013) Thiol-Yne click reactions on alkynyl-dopamine-modified reduced graphene oxide. *Chem Eur J* 19:8673–8678
- [22] Pei S, Cheng H (2012) The reduction of graphene oxide. *Carbon* 50:3210–3228
- [23] Li H, Aulin YV, Frazer L, Borguet E, Kakodkar R, Feser J, Chen Y, An K, Dikin DA, Ren F (2017) Structure evolution and thermoelectric properties of carbonized polydopamine thin films. *ACS Appl Mater Interfaces.* doi:[10.1021/acsami.6b15601](https://doi.org/10.1021/acsami.6b15601)
- [24] Moulder JF, Stickle WF, Sobol PE, Bomben KD (1995) *Handbook of X-ray photoelectron spectroscopy.* Physical Electronics Inc, Chanhassen
- [25] Liu Y, Ai K, Lu L (2014) Polydopamine and its derivative materials: synthesis and promising applications in energy, environmental, and biomedical fields. *Chem Rev* 114:5057–5115
- [26] Li R, Parvez K, Hinkel F, Feng X, Müllen K (2013) Bioinspired wafer-scale production of highly stretchable carbon films for transparent conductive electrodes. *Angew Chem Int Ed* 52:5535–5538